Cell

A Pharmacological Map of the PI3-K Family Defines a Role for p110α in Insulin Signaling

Zachary A. Knight,[1] Beatriz Gonzalez,[4,7] Morri E. Feldman,[1] Eli R. Zunder,[1] David D. Goldenberg,[2] Olusegun Williams,[1] Robbie Loewith,[5] David Stokoe,[3] Andras Balla,[6] Balazs Toth,[6] Tamas Balla,[6] William A. Weiss,[2,3] Roger L. Williams,[4] and Kevan M. Shokat[1,*]

[1] Department of Cellular and Molecular Pharmacology, Howard Hughes Medical Institute
[2] Departments of Neurology and Pediatrics, Neurological Surgery and Brain Tumor Research Center
[3] Comprehensive Cancer Center
University of California, San Francisco, San Francisco, CA 94143, USA
[4] MRC Laboratory of Molecular Biology, Hills Road, Cambridge CB2 2QH, United Kingdom
[5] University of Geneva, Department of Molecular Biology, CH-1211 Geneva 4, Switzerland
[6] Endocrinology and Reproduction Research Branch, National Institute of Child Health and Human Development, National Institutes of Health, Bethesda, MD 20892, USA
[7] Present address: Instituto de Química-Física "Rocasolano" (CSIC), Serrano 119, 28006 Madrid, Spain.
*Contact: shokat@cmp.ucsf.edu
DOI 10.1016/j.cell.2006.03.035

SUMMARY

Phosphoinositide 3-kinases (PI3-Ks) are an important emerging class of drug targets, but the unique roles of PI3-K isoforms remain poorly defined. We describe here an approach to pharmacologically interrogate the PI3-K family. A chemically diverse panel of PI3-K inhibitors was synthesized, and their target selectivity was biochemically enumerated, revealing cryptic homologies across targets and chemotypes. Crystal structures of three inhibitors bound to p110γ identify a conformationally mobile region that is uniquely exploited by selective compounds. This chemical array was then used to define the PI3-K isoforms required for insulin signaling. We find that p110α is the primary insulin-responsive PI3-K in cultured cells, whereas p110β is dispensable but sets a phenotypic threshold for p110α activity. Compounds targeting p110α block the acute effects of insulin treatment in vivo, whereas a p110β inhibitor has no effect. These results illustrate systematic target validation using a matrix of inhibitors that span a protein family.

INTRODUCTION

Phosphoinositide 3-kinases (PI3-Ks) catalyze the synthesis of the phosphatidylinositol (PI) second messengers PI(3)P, PI(3,4)P_2, and PI(3,4,5)P_3 (PIP_3; Fruman et al., 1998). In the appropriate cellular context, these three lipids control diverse physiological processes including cell growth, survival, differentiation, and chemotaxis (Katso et al., 2001). The PI3-K family comprises 15 kinases with distinct substrate specificities, expression patterns, and modes of regulation (Katso et al., 2001). The class I PI3-Ks (p110α, p110β, p110δ, and p110γ) are activated by tyrosine kinases or G protein-coupled receptors to generate PIP_3, which engages downstream effectors such as the Akt/PDK1 pathway, the Tec family kinases, and the Rho family GTPases. The class II and III PI3-Ks play a key role in intracellular trafficking through the synthesis of PI(3)P and PI(3,4)P_2. The PIKKs are protein kinases that control cell growth (mTORC1) or monitor genomic integrity (ATM, ATR, DNA-PK, and hSmg-1).

The importance of these enzymes in diverse pathophysiology has made the PI3-K family the focus of intense interest as a new class of drug targets (Ward et al., 2003). This interest has been fueled by the recent discovery that p110α is frequently mutated in primary tumors (Samuels et al., 2004) and evidence that the lipid phosphatase PTEN, an inhibitor of PI3-K signaling, is a commonly inactivated tumor suppressor (Cantley and Neel, 1999). Efforts are underway to develop small molecule PI3-K inhibitors for the treatment of inflammation and autoimmune disease (p110δ, p110γ, and mTOR), thrombosis (p110β), viral infection (the PIKKs), and cancer (p110α, mTOR, and others). Recently, the first selective inhibitors of these enzymes have been reported (Camps et al., 2005; Condliffe et al., 2005; Jackson et al., 2005; Knight et al., 2004; Lau et al., 2005; Sadhu et al., 2003).

A key challenge in targeting the PI3-K family with drugs is to understand how individual PI3-K isoforms control normal physiology, as this defines the therapeutic window for targeting a specific isoform. Genetic approaches to uncouple the action of PI3-K isoforms have been frustrated by the complex coordinate regulation of these enzymes.

Homozygous deletion of either p110α or p110β (the two most widely expressed PI3-Ks) leads to embryonic lethality in mice (Bi et al., 1999, 2002). Heterozygous deletion of these isoforms is complicated by a compensatory downregulation of the p85 regulatory subunit (Brachmann et al., 2005). Knockout of p85 isoforms induces a paradoxical increase in PI3-K signaling (Ueki et al., 2002, 2003), reflecting the fact that p85 both promotes PI3-K activity (by stabilizing the p110 catalytic subunit) and inhibits it (by reducing basal activity and sequestering essential signaling complexes; Luo et al., 2005; Yu et al., 1998). A similar effect has been observed among the PIKKs, where a deficiency in DNA-PK alters the expression of ATM and hSmg-1 (Peng et al., 2005). In addition to these compensatory mechanisms, PI3-Ks possess kinase-independent signaling activities that can cause inhibitors and knockouts to induce different phenotypes (Knight and Shokat, 2005; Vanhaesebroeck et al., 2005). For example, p110γ knockout mice develop cardiac damage in response to chronic pressure overload, whereas mice bearing a p110γ kinase-dead allele do not (Patrucco et al., 2004). In this case, the difference was traced to an allosteric activation of PDE3B by p110γ that is disrupted in the knockout but unaffected by the kinase-dead allele or an inhibitor.

Cell-permeable small molecule inhibitors make it possible to directly assess the phenotypic consequences of inhibiting a kinase with a drug in a physiologically relevant model system. The challenge for pharmacological target validation is that few well-characterized, selective kinase inhibitors are known. This has been particularly true for the PI3-Ks, as the two primary pharmacological tools available, wortmannin and LY294002, are broadly active within the family. We report here a set of potent, chemotypically diverse small molecule inhibitors that span the PI3-K family. For each compound, we have biochemically enumerated its target selectivity relative to all PI3-K family members and, in many cases, structurally defined its binding mode by X-ray crystallography. Critically, this panel includes representatives from a large number of PI3-K inhibitor chemotypes currently in preclinical drug development and therefore anticipates the biological activities likely to be found in eventual clinical candidates. Using this chemical array, we identify p110α as the key PI3-K activity downstream of the insulin receptor.

RESULTS

A Basis Set of Isoform-Specific PI3-K Inhibitors

Representatives from nine chemical classes of PI3-K inhibitors were selected from compounds under development by the pharmaceutical industry (see Experimental Procedures). Compounds from each class were synthesized and their activity against the class I PI3-Ks measured in vitro. Based on this initial screen, a subset representing the most potent and selective agents was selected for further characterization. This panel includes one to three representatives from each chemical class (Figure 1A and see Figure S1 in the Supplemental Data available with this article online). For most chemotypes, a negative control compound, inactive against all PI3-Ks tested, was also synthesized that differs from the active inhibitor by a single atom substitution (Figure S1).

The extended specificity profile of these compounds was determined by measuring IC_{50} values in vitro against 15 purified PI3-K family members (Figure 1B; Table S1). As this panel includes almost all proteins with sequence homology to p110α, it is highly enriched for the likely targets of these inhibitors. These compounds were also tested against 40 additional purified kinases from three families: the PIPKs, the class II PI4-Ks, and the protein kinases (Tables S1 and S2).

A spectrum of biochemical target selectivities was observed across different inhibitor classes (Figure 1B). The most selective compounds include the quinazolinone purine inhibitors of p110δ (PIK-23, PIK-39, and IC87114), the chromones that target p110β/p110δ (TGX-115, TGX-286, and PIK-108), and the imidazopyridine p110α/p110γ inhibitor PIK-75. At least one compound from each of these chemotypes exhibits >100-fold selectivity between its primary target(s) and other class I PI3-Ks. Other chemical classes (e.g., the aryl thiazolidinones, pyridinylfuranopyrimidines, phenylthiazoles, and imidazoquinazolines; Figure 1A) were found to inhibit multiple PI3-Ks with varied affinities (Figure 1B). These multitargeted compounds possess overlapping yet distinct target selectivities and can complement more selective agents by unmasking hidden synergies between targets within the PI3-K family (Fan et al., 2006).

In several cases, we identified unique targets for these compounds relative to all other inhibitors in our panel. For example, a phenylthiazole, PIK-93, potently inhibits PI4KIIIβ (IC_{50} = 19 nM). This compound is the first potent, synthetic PI4-kinase inhibitor, and we have used this reagent to dissect the role of PI4-K isoforms in calcium signaling (Z.A.K., K.M.S., P. Varnai, A.B., and T.B., unpublished data). Similarly, the pyridinylfuranopyrimidine PI-103 potently inhibits both the rapamycin-sensitive (mTORC1, IC_{50} = 20 nM) and rapamycin-insensitive (mTORC2, IC_{50} = 83 nM) complexes of the protein kinase mTOR. Thus, PI-103 represents the first potent, synthetic mTOR inhibitor.

Discovery of Pharmalogs within the PI3-K Family

More than a decade of research on protein kinase inhibitors has revealed trends in inhibitor sensitivity among kinases (SAR homology) and target selectivity among chemotypes (target homology) that are critical to predicting off-target effects and interpreting inhibitor-induced phenotypes (Knight and Shokat, 2005). To better understand the relationships between PI3-K-related targets and chemotypes, we subjected family-wide specificity data to principal component analysis (Figure 1C). This analysis reorganizes the multidimensional relationship between inhibitors and their targets into principal components that can be plotted to depict the relatedness of these elements. Representing the data in this way can reveal

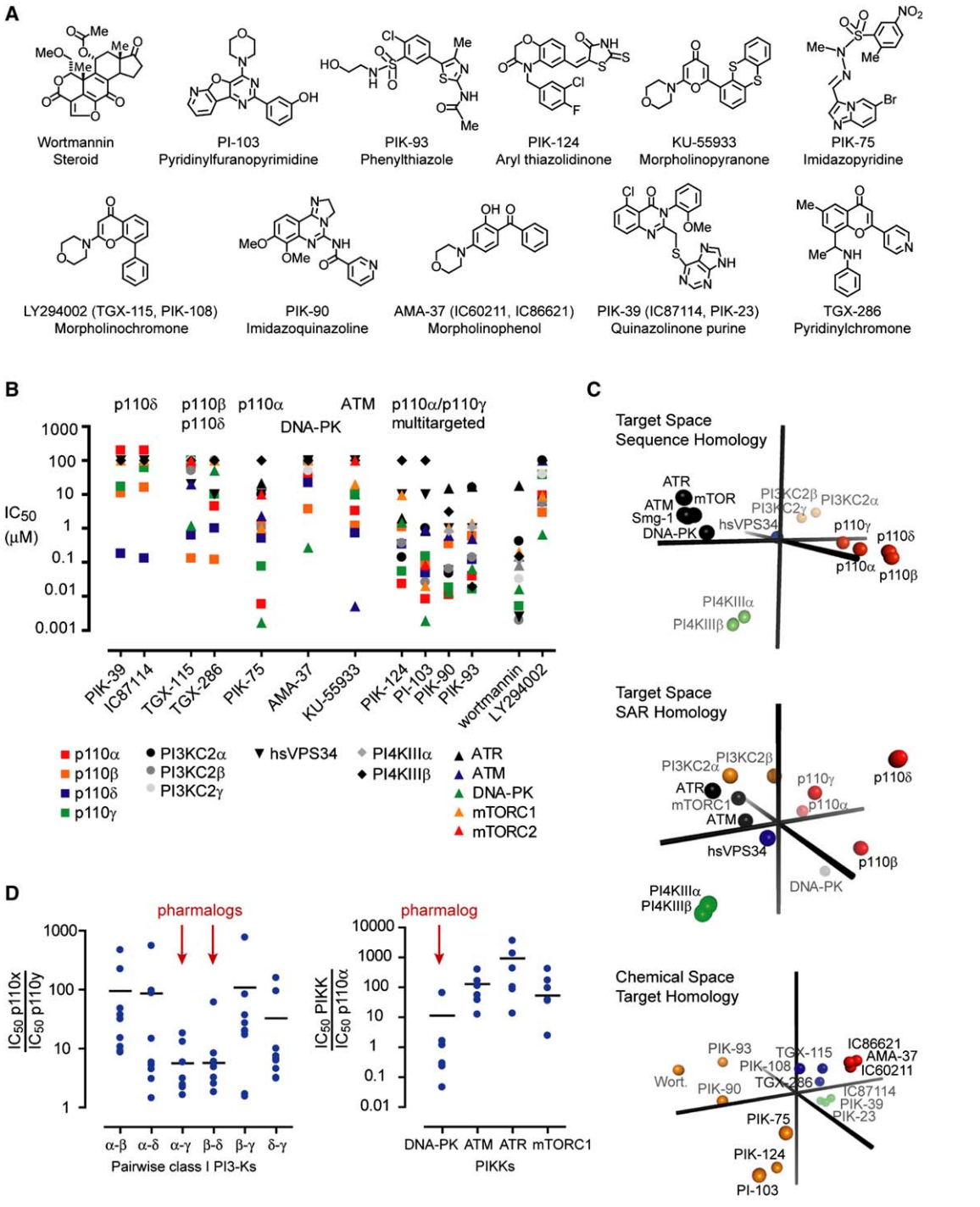

Figure 1. Biochemical Analysis of Selected PI3-K Inhibitors

(A) Structures of representative compounds from eleven classes of PI3-K inhibitors.

(B) Distribution of IC_{50} values for selected inhibitors against PI3-K family members. Some IC_{50} values for AMA-37 and TGX-115 have been reported previously (Knight et al., 2004).

(C) Principal component analysis of the relationships between PI3-Ks and inhibitors. (Top) Plot of the similarity between PI3-Ks according to their sequency identity within the kinase domain. (Middle) Plot of the similarity between PI3-Ks according to their IC_{50} values against small molecule inhibitors. (Bottom) Plot of the similarity between inhibitors based on their IC_{50} values against PI3-Ks.

(D) (Left panel) The ratio of IC_{50} values for one compound from each chemotype (TGX-115, AMA-37, PIK-39, PIK-75, PIK-90, PIK-93, PI-103, PIK-124) against pairs of class I PI3-Ks. (Right panel) The ratio of IC_{50} values for one compound from each chemotype with an $IC_{50} < 5$ μM against p110α between PIKKs and p110α. Blue dots represent compounds and bars represent the geometric mean of these ratios.

functional similarities between the ATP binding pockets of kinases or between chemotypes of inhibitors that cannot be predicted from the sequence of the kinase or the chemical structure of the inhibitor.

We first compared PI3-K family members according to their sensitivity to different inhibitors (Figure 1C, center) and contrasted this with the same analysis based on pairwise sequence homology within the kinase domain (Figure 1C, top). Analysis by sequence segregates the PI3-K family into five clusters, recapitulating the original assignment of these enzymes into subfamilies based on sequence similarity (Domin and Waterfield, 1997). When these kinases are instead clustered by inhibitor sensitivity, several key differences emerge. First, the class I PI3-Ks are more widely distributed by SAR homology than by sequence homology. This reflects the fact that the compounds in our panel distinguish between these kinases to a greater extent than sequence differences would predict. Nonetheless, SAR homology persists among the class I PI3-Ks. p110β and p110δ cluster in target space (Figure 1C, center), and compounds that inhibit p110β tend to inhibit p110δ more potently than other PI3-Ks (Figure 1D, left). Likewise, p110α tends to be inhibited by compounds targeting p110γ and vice versa (Figure 1D, left). We refer to the pairs p110β/p110δ and p110α/p110γ as pharmalogs in recognition of this SAR homology and suggest that it may be more challenging to find inhibitors with high selectivity between these targets. Consistent with this prediction, the recently described p110γ inhibitor AS604850, which was not included in our analysis, has been reported to inhibit p110α more potently than p110β or p110δ (Camps et al., 2005).

A second unexpected result from this analysis is that p110α clusters in target space with DNA-PK based on SAR homology (Figure 1C, center), even though these kinases share limited sequence identity (Figure 1C, top). Indeed, five of the six chemotypes that inhibit p110α with an $IC_{50} < 5$ μM also potently inhibit DNA-PK (Figure 1D, right). By contrast, other PIKKs such as mTOR, ATM, and ATR are less sensitive to these same compounds (Figure 1D, right). This suggests that DNA-PK inhibition is a common feature of p110α inhibitors and likely reflects a cryptic similarity between the active sites of these two pharmalogs.

We next analyzed compounds according to their target selectivity in order to reveal relationships within and among chemotypes. Compounds from a single chemotype cluster based on target homology (Figure 1C, bottom), defining the regions of chemical space occupied by p110δ inhibitors (green), p110β inhibitors (blue), DNA-PK inhibitors (red), and p110α/multitargeted inhibitors (orange). By including the panspecific natural product wortmannin as a reference point, this analysis highlights the selectivity continuum among inhibitors that target p110α.

Structures of Isoform-Specific PI3-K Inhibitors

To better understand the selectivity trends observed among these chemically diverse inhibitors, the structural basis for their binding to PI3-K was investigated. Crystal structures of p110γ have been reported, alone and in complex with ATP or panspecific inhibitors such as LY294002 and wortmannin (Walker et al., 2000; Walker et al., 1999). To explore how potent and selective inhibitors bind, the crystal structures of PI3-K inhibitors from three chemotypes bound to human p110γ were determined at 2.5–2.6 Å resolution: the quinazolinone purine PIK-39, the imidazoquinazoline PIK-90, and the phenylthiazole PIK-93 (Figure 2; Table S3; Movies S1 and S2).

Based on these cocrystal structures and a conserved arylmorpholine pharmacophore model, structural models were generated for three additional chemotypes bound to p110γ: the pyridinylfuranopyrimidine PI-103, the morpholinochromone PIK-108, and the morpholinopyranone KU-55933 (Figure 2; Movies S1–S4). Model-building for these inhibitors was guided by the observation that each compound contains the key arylmorpholine pharmacophore found in LY294002. The oxygen atom in the morpholine ring of LY294002 makes a critical hydrogen bond to the backbone amide of Val 882 (p110γ numbering) and substitution of this oxygen abolishes LY294002 binding to PI3-K (Walker et al., 2000). In a similar fashion, we (Figure S1) and others (Hickson et al., 2004) have shown that replacement of the morpholine oxygen atom in these compounds abolishes PI3-K inhibition, supporting a conserved mode of binding for the arylmorpholine moiety in these inhibitors.

A Conformational Switch that Controls Inhibitor Selectivity

The discovery of compounds that can distinguish between closely related isozymes remains a major challenge for kinase-inhibitor design. The most selective PI3-K inhibitor reported here, PIK-39, is a quinazolinone purine that inhibits p110δ at midnanomolar concentrations, p110γ and p110β at concentrations ~100-fold higher, and shows no activity against any other PI3-K family member, including p110α, at concentrations up to 100 μM (Table S1). The remarkable biochemical selectivity of this compound is achieved through an unusual binding mode revealed in its cocrystal structure with p110γ (Figure 2C). Only the mercaptopurine moiety of PIK-39 makes contacts within the interior of the ATP binding pocket, and this ring system is rotated ~110° and twisted ~35° out of the plane relative to the adenine of ATP. In this orientation, PIK-39 satisfies hydrogen bonds to the backbone amides of Val 882 and possibly Glu 880 (thereby recapitulating the hydrogen bonds made by N1 and N6 of adenine).

In contrast to other PI3-K inhibitor structures, PIK-39 does not access the deeper pocket in the active site interior (Figure 2C, yellow). Instead, the quinazolinone moiety of PIK-39 extends out to the entrance of the ATP binding pocket (Figure 2B). In this region, the kinase accommodates the inhibitor by undergoing a conformational rearrangement in which Met 804 shifts from an "up" position, in which it forms the ceiling of the ATP binding pocket, to a "down" position, which it packs against the quinazolinone moiety (Movie S2). The effect of this movement,

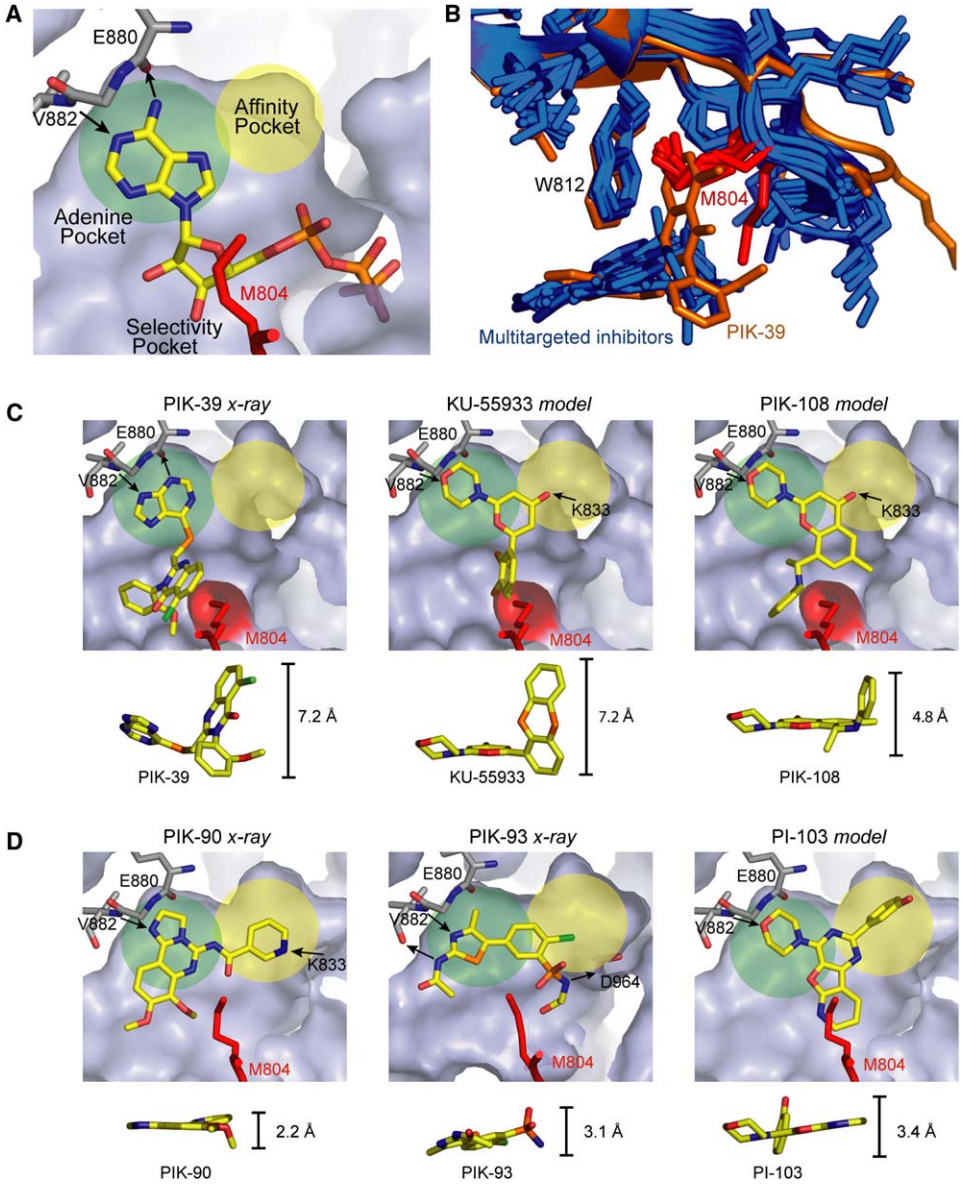

Figure 2. Structures of Isoform-Selective PI3-K Inhibitors

(A) Crystal structure of ATP in the active site of p110γ, highlighting regions designated as the adenine, affinity, and selectivity pockets. Hydrogen bonds are indicated by arrows.

(B) Alignment of all reported PI3-K inhibitor cocrystal structures. PIK-39 is colored orange and all other inhibitors are colored blue. Met 804 (red) adopts an up conformation in all structures except PIK-39.

(C) Crystal structures and models of isoform-selective PI3-K inhibitors bound to p110γ.

(D) Crystal structures and models of multitargeted PI3-K inhibitors bound to p110γ.

which is unique to the PIK-39 structure (Figure 2B), is to create a novel hydrophobic pocket between Met 804 and Trp 812 at the entrance to the ATP binding site. This induced-fit pocket buries ~180 Å^2 of solvent accessible inhibitor surface area, enabling PIK-39 to achieve nanomolar affinity despite limited contacts within the active site core.

Since the class IA PI3-Ks have no sequence differences in the adenine pocket (Knight et al., 2004), the selectivity of PIK-39 cannot be explained by sequence variation within this region. By contrast, the conformational rearrangement observed in our crystal structure suggests a mechanism for the selectivity of this chemotype, since different PI3-K isoforms may exhibit differential conformational plasticity in the region surrounding Met 804. In this regard, Met 804 is located within a loop in the catalytic domain that is structurally analogous to the glycine-rich loop of protein kinases. In protein kinases, this loop is unusually flexible, and its dynamics appear to optimally align ATP

relative to the peptide substrate (Madhusudan et al., 1994). Movement of Met 804 in the PIK-39 structure induces a shift in the peptide backbone that propagates through this loop connecting β strands kβ3 and kβ4 and into the adjacent α helix kα2. These regions possess low sequence identity among the class I PI3-Ks, and this distal sequence variation may account for differential conformational plasticity among isoforms. This mode of inhibitor binding is reminiscent of selective protein kinase inhibitors such as imatinib that exploit differentially accessible conformational states among closely related paralogs (Schindler et al., 2000).

The unexpected conformational mobility of Met 804 in the PIK-39 structure prompted us to ask whether other selective inhibitors may rely on this same feature. Two of the most selective chemotypes in our panel are the chromones that target p110β/p110δ (e.g., TGX-115 and PIK-108) and the pyranone KU-55933 that targets ATM. Modeling based on the LY294002 structure suggests that these compounds project large aromatic substituents toward the induced pocket observed in the PIK-39 structure (Figure 2C; Movies S3 and S4). Therefore, it is possible that these compounds also achieve their selectivity through unique interactions in this region, either by occupying a similar induced pocket (PIK-108—Figure S2 and Movie S3) or by exploiting natural sequence differences at this position (KU-55933—Figure S3 and Movie S4).

A Deeper Affinity Pocket that Controls Inhibitor Potency

Several compounds in our panel potently inhibit multiple PI3-K family members, and we sought to understand how these inhibitors achieve high affinity, panspecific binding. As PIK-90 and PIK-93 are the two most potent and multitargeted synthetic PI3-K inhibitors that have been reported (Figure 1), we determined cocrystal structures of these compounds bound to p110γ.

PIK-90 and PIK-93 both make a hydrogen bond to the backbone amide nitrogen of Val 882 (Figure 2D), an interaction conserved among all known PI3-K inhibitors (Walker et al., 2000). In addition to this hydrogen bond, PIK-93 makes a second hydrogen bond to the backbone carbonyl of Val 882 and a third between its sulphonamide moiety and the side chain of Asp 964. PIK-93 is one of the most polar inhibitors in our panel (CLogP = 1.69), and these extended polar interactions may compensate for its limited hydrophobic surface area.

PIK-90 binds in a mode similar to PIK-93, although this larger compound makes more extensive hydrophobic interactions, burying 327 Å^2 of solvent-accessible surface area. To achieve this, PIK-90 projects its pyridine ring into a deeper cavity that is partially accessed by PIK-93 but not occupied by ATP (Figure 2D, yellow). In this region, the pyridine ring of PIK-90 is poised to make a hydrogen bond to Lys 833, and we find that replacement of this pyridine nitrogen with carbon results in a 100-fold loss in affinity (PIK-95, Figure S1). PI-103, a third multitargeted PI3-K inhibitor, projects a phenol into the same pocket based on an arylmorpholine pharmacophore model (Figure 2D).

Two structural features distinguish these potent, multitargeted inhibitors from the more selective compounds in our panel. First, these compounds adopt a flat conformation in the ATP binding pocket, whereas highly selective inhibitors project out of the plane occupied by ATP (Figure 2). Second, the most potent inhibitors project into a deeper binding pocket that is not accessed by ATP (Figure 2A). Much of the surface of this affinity pocket is contributed by the side chain of Ile 879, a residue that we have argued is structurally analogous to the gatekeeper residue in protein kinases (Alaimo et al., 2005). Interactions in this region may play an analogous role in the binding of high-affinity lipid kinase inhibitors.

Probing the Selectivity and Affinity Pockets

The inhibitor structures reported here are in complex with p110γ, the only PI3-K whose structure has been solved. It is possible that selective compounds (e.g., PIK-39) bind in a different orientation when complexed with their highest affinity target (e.g., p110δ), even though these kinases display a high degree of sequence conservation within the ATP binding pocket. We therefore performed a series of experiments to probe the binding mode of these compounds and also test the prediction that distinct regions of the ATP binding pocket contribute to inhibitor selectivity and affinity.

A confounding SAR of quinazolinone purines such as PIK-39 is that the mercaptopurine moiety can be replaced with adenine (Figure S1, compare PIK-39 and IC87114) without significantly altering the potency or selectivity of these compounds, despite the fact that this substitution dramatically alters the shape and hydrogen bonding potential of the inhibitor. To understand how this is possible, we replaced the mercaptopurine in our PIK-39 structure with adenine to yield a model of IC87114 (Figure 3A). Remarkably, this substitution situates the adenine of IC87114 in the correct orientation to make the same hydrogen bonds as the mercaptopurine of PIK-39, even though these two ring systems are rotated by 110° with respect to each other. Thus, the PIK-39 cocrystal structure directly explains an unusual SAR of this chemotype, supporting a conserved binding mode for these inhibitors.

Unlike other inhibitor chemotypes, PIK-39 does not exploit the deeper-affinity pocket within the ATP binding site (Figure 2C). To probe the importance of this region in controlling inhibitor affinity, we sought to design a more potent analog of PIK-39 that does access this pocket. PIK-39 itself does not possess a suitable site for chemical derivatization in this region, but modeling indicates that by replacing the adenine of IC87114 with the isosteric pyrazolopyrimidine (PIK-293, Figure 3A), aromatic substituents may be projected from C3 of this compound into the affinity pocket. We therefore synthesized the pyrazolopyrimidine analog of IC87114 (PIK-293) as well as a novel analog that contains a *m*-phenol at this position (PIK-294, Figure 3A). PIK-294 was designed, in part, based on the

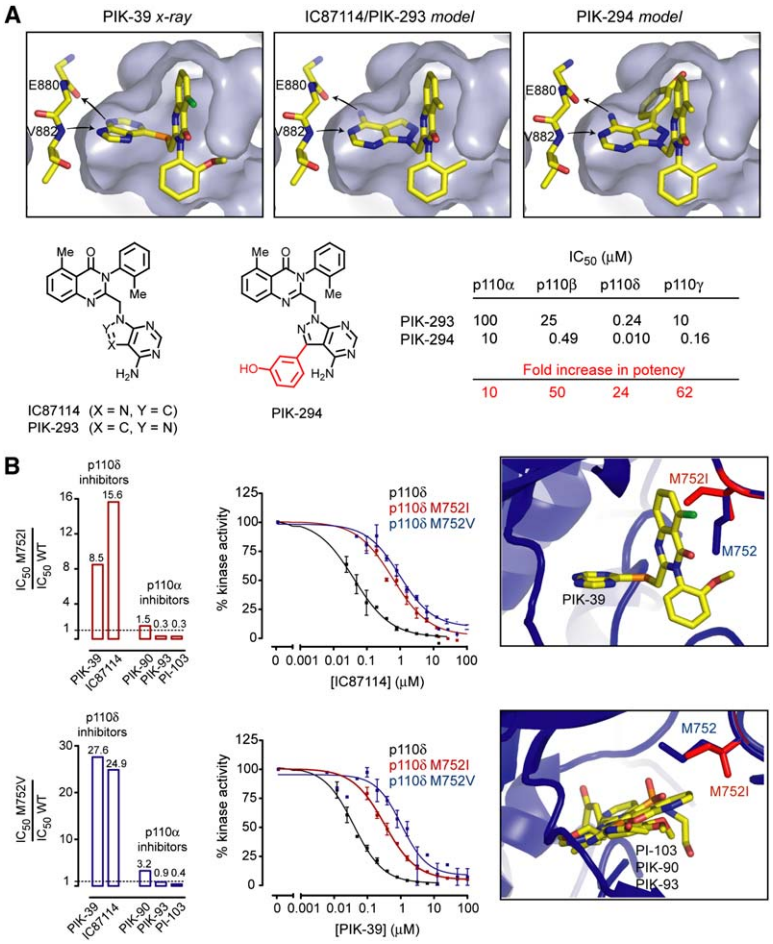

Figure 3. Probing the Selectivity and Affinity Pockets

(A) (Top panel) Structure of PIK-39 bound to p110γ and predicted binding mode for IC87114, PIK-293 and PIK-294. Hydrogen bonds are indicated by arrows. (Lower panel) PIK-294 projects a *m*-phenol (red) into the affinity pocket, and this compound is more potent against the class I PI3-Ks.

(B) (Left panel) Ratio of IC_{50} values for inhibition of mutant and wild-type p110δ. (Center panel) Dose-response curves for inhibition of wild-type, M752I, and M752V p110δ by IC87114 and PIK-39. Error bars represent mean ± SEM. (Right panel) Binding modes of PIK-39 (top) and multitargeted inhibitors (bottom) relative to the Met 752 mutation (red) that differentially perturbs the binding of these inhibitors.

observation that one of the most potent inhibitors in our panel (PI-103) also projects a *m*-phenol into this region (Figure 2D). These compounds were then tested for inhibition of the class I PI3-Ks. We find that PIK-294 is 20- to 60-fold more potent than the parent compound, PIK-293, making PIK-294 one of the most potent p110δ-selective inhibitors that has been reported (Figure 3A). The successful design of this compound supports a conserved binding orientation for this chemotype across all PI3-Ks.

The structure of PIK-39 bound to p110γ revealed a conformational rearrangement of Met 804 to create an induced pocket, and we have hypothesized that this conformational rearrangement underlies the selectivity of PIK-39 for p110δ. A prediction of this model is that mutation of Met 804 should perturb the binding of p110δ-selective inhibitors (which access the induced pocket), but not affect other classes of inhibitors (which do not access this pocket). Modeling suggests that mutation of Met 804 to a β-branched amino acid (such as valine or isoleucine) should restrict the pocket formed by rearrangement of that residue (Figure 3B, right). Therefore, we mutated the corresponding residue in p110δ (Met 752) to valine or isoleucine, expressed and purified these kinases and tested them for sensitivity to PI3-K inhibitors (Figure 3B). We find that M752I and M752V p110δ are resistant to the p110δ-selective inhibitors PIK-39 and IC87114 but retain sensitivity to the p110α/multitargeted inhibitors PIK-90, PIK-93, and PI-103. This chemotype-specific resistance supports the unique role of Met 752 in gating an inducible selectivity pocket.

The Role of PI3-K Isoforms in Insulin Signaling

Class I PI3-Ks are activated by the insulin receptor (Ruderman et al., 1990), and PI3-K activity is required for the metabolic effects of insulin (Katso et al., 2001). The central role of PI3-K in insulin signaling raises the possibility that therapeutic use of PI3-K inhibitors may cause insulin resistance and associated morbidity. Broad spectrum pharmacological inhibition of all PI3-Ks would be predicted to block the metabolic effects of insulin, although this has not been demonstrated in vivo. While it may be possible to selectively inhibit individual PI3-K isoforms without impairing glucose homeostasis, the sensitivity of this process to pharmacological inhibition of each class I PI3-K remains to be defined. Asano and coworkers have argued that p110β is the primary insulin-responsive PI3-K in adipocytes, relying largely on adenoviral overexpression of p110 isoforms and microinjection of isoform-specific

inhibitory antibodies (Asano et al., 2000). These pioneering studies were among the first to explore signaling by PI3-K isoforms, but it is unclear to what extent these approaches can anticipate the effects of small molecule inhibitors. The use of knockout animals to study the role of p110 isoforms in insulin signaling has been complicated by the inability to generate viable homozygotes and a compensatory down-regulation of the p85 subunit that is observed in heterozygous animals (Brachmann et al., 2005). For these reasons, the key translational question with respect to insulin signaling by PI3-K—the sensitivity of this process to pharmacological inhibition of each isoform—remains unresolved. We therefore chose to examine this question using isoform-selective PI3-K inhibitors.

p110α Is the Primary Insulin Responsive PI3-K in Adipocytes and Myotubes

We initially explored the effects of PI3-K inhibitors in 3T3-L1 adipocytes and L6 myotubes, two widely used model systems for studying insulin action in fat and muscle, respectively. Activation of the PI3-K pathway was monitored by Western blotting for phosphorylation of known PI3-K effectors (Figure 4A) and cellular inositol lipids were quantified by ^{32}P-orthophosphate metabolic labeling (Figure 4B).

All p110α inhibitors potently blocked insulin-stimulated phosphorylation of Akt in adipocytes and myotubes (Figures 4 and S4). This was observed for multitargeted inhibitors such as PIK-90 and PI-103 (which inhibit p110α most potently but also target p110β at concentrations 10 to 30-fold higher) as well as PIK-75, which inhibits p110α >200-fold more potently than p110β. p110α inhibitors also blocked activation of the mTORC1 pathway as measured by phosphorylation of p70S6K and its target, rpS6. Phosphorylation of the mTORC1 target 4E-BP1 was not insulin stimulated, and consequently 4E-BP1 phosphorylation was only blocked by PI-103, which directly inhibits mTORC1 (Figure S1). Consistent with their effect on pathway effectors, PIK-75 and PI-103 also potently blocked production of PI(3,4)P_2 and PIP_3 in adipocytes and PIP_3 in myotubes (PI(3,4)P_2 was not detected in myotubes).

By contrast, inhibitors of p110β (TGX-115 and TGX-286) and p110δ (IC87114 and PIK-23) had no effect on the insulin-stimulated phosphorylation of any protein in the PI3-K pathway (Figures 4 and S4). Strikingly, the p110β inhibitor TGX-115 reduced insulin-stimulated PI(3,4)P_2 and PIP_3 levels in adipocytes by ~50%, yet failed to block Akt or mTORC1 activation in these cells (Figure 4). However, TGX-115 and TGX-286 did potently inhibit Akt phosphorylation induced by lysophosphatidic acid (Figure 4C), a stimulus that activates p110β (Yart et al., 2002), confirming that these inhibitors can functionally block p110β activity in these cells. These data argue that p110β and p110δ play a less-significant role in insulin signaling in adipocytes and myotubes.

Several compounds in our panel inhibit PIKKs as a secondary target to PI3-K inhibition, and recent reports suggest these kinases may play a role in Akt activation (Feng et al., 2004; Viniegra et al., 2005). We find that neither the DNA-PK inhibitor AMA-37 nor the ATM inhibitor KU-55933 blocks insulin-stimulated activation of the PI3-K pathway in these cells (Figure S4), suggesting that these targets are unlikely to contribute to the differential effects of PI3-K inhibitors in our panel.

Functional Inhibition of Glucose Transport in Cells and Animals

We next investigated whether biochemical inhibition of the PI3-K pathway by these inhibitors induces functional inhibition of glucose transport in cells and animals. We find that p110α inhibitors blocked insulin-stimulated glucose uptake in adipocytes with a dose response that closely mirrors their ability to block Akt phosphorylation (Figure 5A). By contrast, the p110β inhibitor TGX-115 had no effect on glucose transport, whereas TGX-286 had a small effect at the highest dose; we attribute this weak activity of TGX-286 to p110α inhibition at high concentrations, as this compound is less selective than TGX-115 (Table S1).

We next tested whether the effects of these inhibitors in cell culture are recapitulated in vivo by performing insulin tolerance tests in mice. Animals were fasted to normalize blood glucose levels and then challenged with insulin or vehicle (PBS) by intravenous injection. Immediately following insulin treatment, mice were given inhibitor (10 mg/kg PI-103, PIK-90, or TGX-115) or vehicle (50% DMSO) by intraperitoneal injection, and blood glucose levels were monitored at 15 min intervals. Treatment with insulin alone induced a decline in blood glucose levels by ~80% over 1 hr (Figure 5B, red). Strikingly, PI-103 completely protected animals from this insulin-stimulated decline in blood glucose, while PIK-90 was almost as effective (Figure 5B). By contrast, the p110β/p110δ inhibitor TGX-115 had no effect on blood glucose levels in response to insulin (Figure 5B). These data are consistent with our results from cell-based experiments which argue that p110α is the primary PI3-K that mediates the acute effects of insulin.

p110α Is the Primary Lipid Kinase in the IRS-1 Complex

p110β and p110δ inhibitors fail to block insulin signaling in myotubes or adipocytes, but this does not imply that these isoforms make no contribution to insulin signaling in these cells. We therefore sought to identify a role for p110β and p110δ in this pathway through a more quantitative analysis of the contribution of each isoform.

Western blotting confirmed that p110α and p110β are expressed in adipocytes, whereas p110α, p110β, and p110δ are expressed in myotubes (Figure 6D). The kinase activity of immunoprecipitated p110α and p110β was increased by insulin treatment, and the relative activity of each isoform was consistent with our finding that p110α is the dominant kinase in intact cells (Figure 6C).

PI3-K is recruited to the insulin receptor by the insulin receptor substrate (IRS) proteins. We therefore analyzed the activity of each PI3-K isoform in the IRS-1 complex.

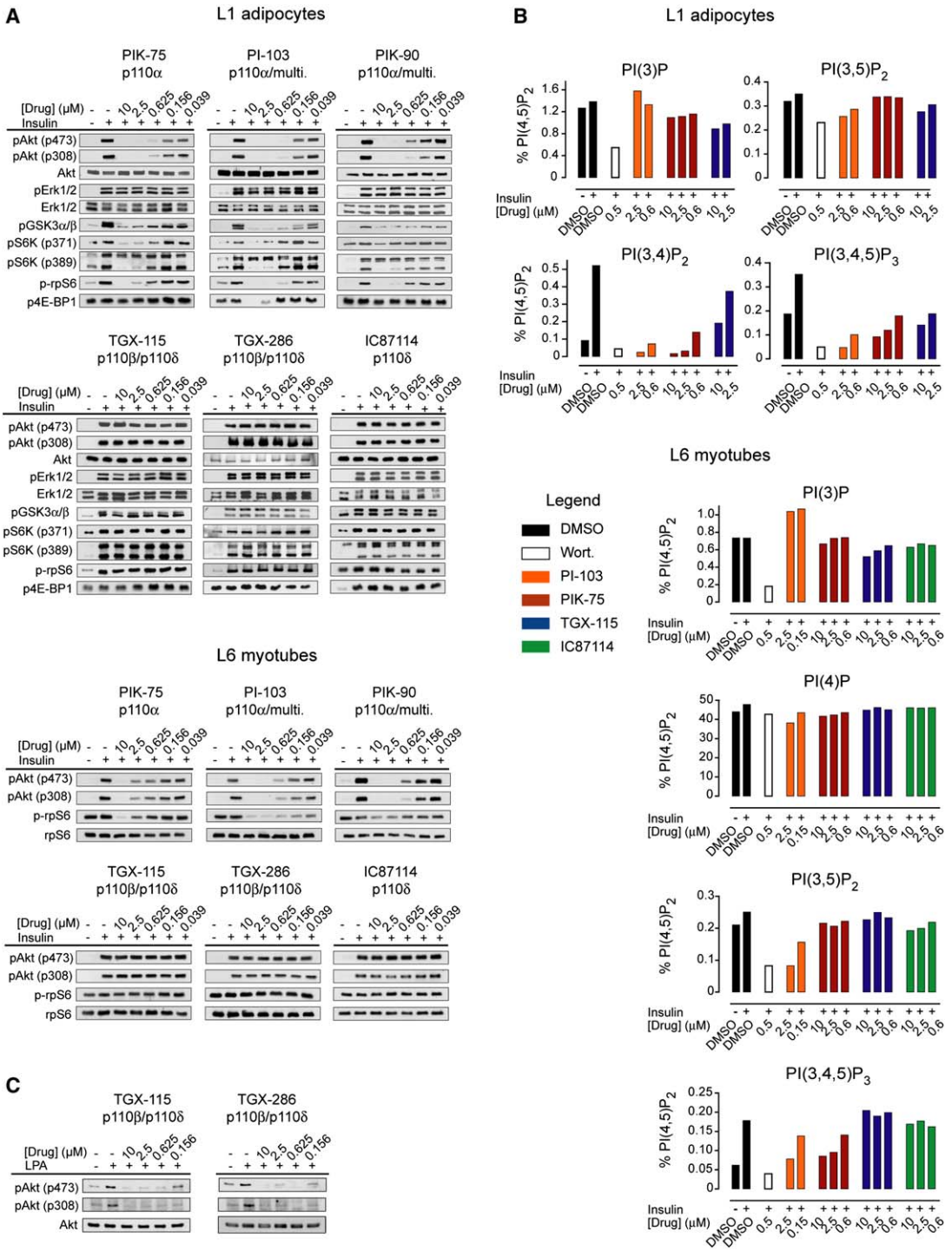

Figure 4. Biochemical Analysis of the PI3-K Pathway in Fat and Muscle Cells

(A) Western blots of lysates from 3T3-L1 adipocytes or L6 myotubes stimulated with insulin (100 nM) in the presence of PI3-K inhibitors. Phosphorylation sites not specified in the figure: ERK1/2 (p202/204), GSK3α/β (p21/9), rpS6 (p235/236), 4E-BP1 (p37/46).

(B) Inositol lipid levels following insulin stimulation (100 nM) in the presence of PI3-K inhibitors.

(C) Western blots of lysates from L6 myotubes stimulated with LPA (10 μM) in the presence of PI3-K inhibitors.

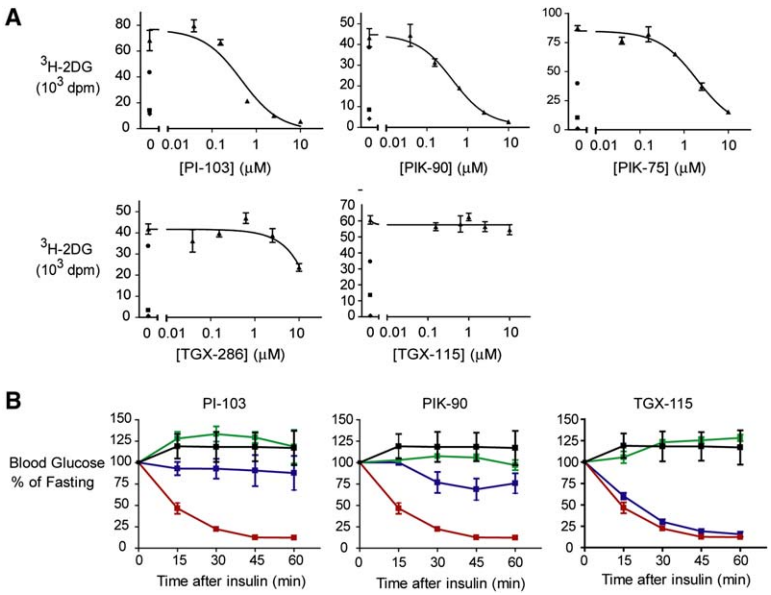

Figure 5. Effect of Inhibitors on Glucose Transport in Adipocytes and Mice

(A) Insulin-stimulated transport of ^{3}H-2-deoxyglucose into adipocytes. Triangle, insulin plus inhibitor; square, no insulin; diamond, insulin plus cytochalasin B (20 μM); circle, 1% of input ^{3}H-2-deoxyglucose. Error bars represent mean ± SEM.

(B) Insulin tolerance tests in mice. Red, insulin plus drug vehicle; blue, insulin plus drug; green, drug plus insulin vehicle; black, insulin vehicle plus drug vehicle. Error bars represent mean ± SEM.

To do this, an assay was developed to quantitate the contribution of each class IA PI3-K isoform to the total PI3-K activity present in protein complexes that may contain multiple lipid kinases. This assays relies on the ability of three compounds in our panel (PIK-23, TGX-115, and PIK-75) to inhibit greater than 90% of the activity of their primary target, with minimal inhibition of the other class IA PI3-Ks, at a selected concentration of drug in vitro (Figure 6A). Adipocytes and myotubes were stimulated with insulin, IRS-1 was immunoprecipitated from lysates of these cells, and immunocomplexes were subjected to an in vitro PI3-K assay (Figure 6B). IRS-1 associated PI3-K activity increased 20- to 40-fold within 90 s of insulin stimulation in each cell type and then gradually declined over 30 min (Figure 6B, blue). Treatment with the p110α inhibitor PIK-75 dramatically reduced the overall level of PI3-K activity in immunoprecipitates from both cells (Figure 6B, green). By contrast, the p110β/p110δ inhibitor TGX-115 reduced IRS-1-associated PI3-K activity by ~30% in adipocytes and ~10% in myotubes (Figure 6B, red line). The p110δ inhibitor PIK-23 had no effect on IRS-1-associated PI3-K activity from adipocytes, and a small effect in myotubes (Figure 6B, black). These data are consistent with our findings from intact cells that insulin stimulated PIP_3 production is most sensitive to p110α inhibitors and that p110β inhibitors partially block PIP_3 production in adipocytes, but not in myotubes.

These data suggest that p110β associates with IRS-1 in adipocytes and generates PIP_3, but that this pool of PIP_3 is not functionally coupled to Akt activation. As PI3-K also controls a retrograde signaling pathway which leads to the phosphorylation of IRS-1 on serine residues that target this protein for degradation (Harrington et al., 2005), we next explored the isoform dependence of this process. Adipocytes were treated with isoform-specific inhibitors, stimulated with insulin for 30 min, and IRS-1 was immunoprecipitated from lysates of these cells and blotted for phosphorylation of three residues (Ser 307, Ser 612, and Ser 632). Phosphorylation of these residues is insulin stimulated, wortmannin sensitive, and promotes IRS-1 inactivation, indicating that these are major sites of negative regulation under the control of the PI3-K pathway. We find that inhibitors of p110α, but not inhibitors of p110β/p110δ, abolish the phosphorylation of these sites (Figure 6E).

p110β/p110δ Set a Phenotypic Threshold in Myotubes, but Not Adipocytes

It is possible that p110β or p110δ contributes a pool of PIP_3 that is not independently required for Akt phosphorylation but which defines a threshold for the amount of p110α activity necessary to activate the pathway. A prediction of this model is that inhibition of p110β or p110δ should shift the amount of p110α activity required to activate Akt and other downstream effectors.

We tested this hypothesis by measuring the effect of the p110β/p110δ inhibitor TGX-115 on the ability of the p110α inhibitor PIK-75 to block Akt phosphorylation at Thr 308. TGX-115 alone at concentrations up to 10 μM had no effect on insulin-stimulated Thr 308 phosphorylation in either adipocytes or myotubes (Figure 7A, black). PIK-75 alone blocked Thr 308 phosphorylation in these two cell types with IC_{50} values of 1.2 and 1.3 μM, respectively (Figure 7A, blue). When PIK-75 was retested in the presence of 10 μM TGX-115, the dose response in myotubes shifted to ~8-fold lower concentrations (IC_{50} = 0.17 μM); an identical dose shift was observed for phosphorylation of Akt Ser 473 (Figure S5). By contrast, no significant shift was observed in adipocytes (Figure 7A, red).

These results support a model in which p110β/p110δ synthesize a basal pool of PIP_3 in myotubes that lowers the amount of p110α activity required for Akt phosphorylation; the change in this phenotypic threshold is detected

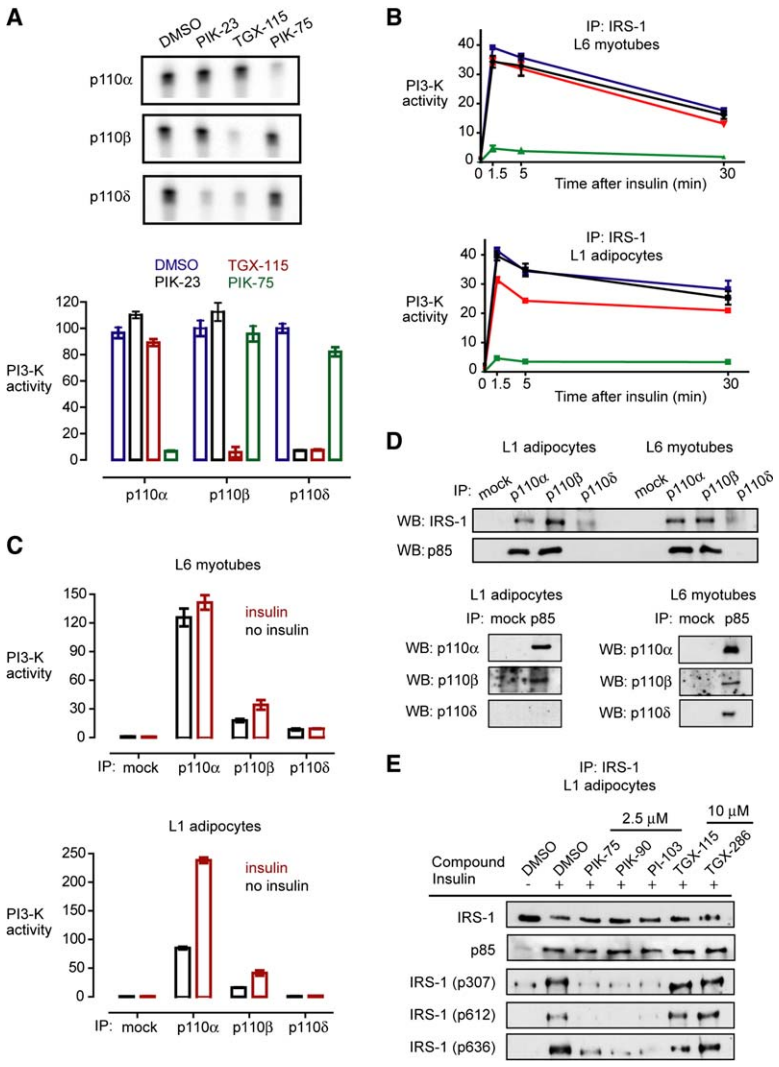

Figure 6. p110α Is the Dominant PI3-K Activity Associated with the IRS-1 Complex

(A) Inhibition of purified class I PI3-Ks by PIK-23 (1.5 μM), TGX-115 (1.5 μM), and PIK-75 (0.05 μM) in vitro in the presence of 10 μM ATP. Error bars represent mean ± SEM.

(B) Relative PI3-K activity associated with IRS-1 immunoprecipitates at 1.5, 5, and 30 min after stimulation with insulin (100 nM). Kinase reactions were performed in the presence of DMSO (blue), 1.5 μM PIK-23 (black), 1.5 μM TGX-115 (red), or 0.05 μM PIK-75 (green). Error bars represent mean ± SEM.

(C) PI3-K activity associated with immunoprecipitates of the catalytic subunits of class IA enzymes from cells with and without prior insulin stimulation (100 nM, 90 s). Error bars represent mean ± SEM.

(D) (Top panel) Western blots for IRS-1 and p85 from immunoprecipitates of each class IA PI3-K. (Bottom panel) Western blot for class IA PI3-Ks from immunoprecipitates of p85.

(E) Western blot for IRS-1, p85, and phosphorylated Ser 307, Ser 612, or Ser 636 of IRS-1 from adipocytes treated with insulin (100 nM, 30 min).

as a shift in the dose-response curve for the p110α inhibitor PIK-75. Nonetheless, we did not observe a significant decrease in bulk PIP_3 levels in myotubes in response TGX-115 treatment (Figure 4B). This may reflect the difficulty in quantifying small changes in PIP_3 levels by metabolic labeling or the fact that only certain pools of PIP_3 are functionally coupled to Akt phosphorylation.

We reasoned that one way to provide support for this model would be to use an inhibitor of PTEN to acutely unmask basal PIP_3 synthesis. Treatment with the PTEN inhibitor bpV(pic) (Schmid et al., 2004) induced rapid Akt phosphorylation in both myotubes and adipocytes, and the inhibitor sensitivity of this Akt phosphorylation was measured (Figure 7B). p110β inhibitors potently blocked this Akt phosphorylation in myotubes but had no effect in adipocytes (Figure 7B). This is consistent with our findings from dose-shift experiments and supports a model in which p110β generates a basal pool of PIP_3 that is coupled to Akt phosphorylation in myotubes.

DISCUSSION

The PI3-K pathway is the most frequently activated signaling pathway in human cancer. For this reason, PI3-K inhibitors will likely to follow protein kinase inhibitors as the next major class of targeted drugs. In contrast to protein kinases, however, the structural requirements for potent and selective PI3-K inhibition have not been defined. It is likewise unknown which PI3-Ks should be targeted for many diseases and to what extent inhibition of these kinases will impair normal physiology. These uncertainties reflect the unique challenges facing target validation for this family of enzymes, which are coordinatively regulated and control complex biology. As multiple PI3-K isoforms are often recruited to a single protein complex where they phosphorylate the same substrate, quantitative differences in thresholds and timing of catalytic activity are likely to be critical in defining the phenotypic consequences of inhibiting distinct PI3-Ks.

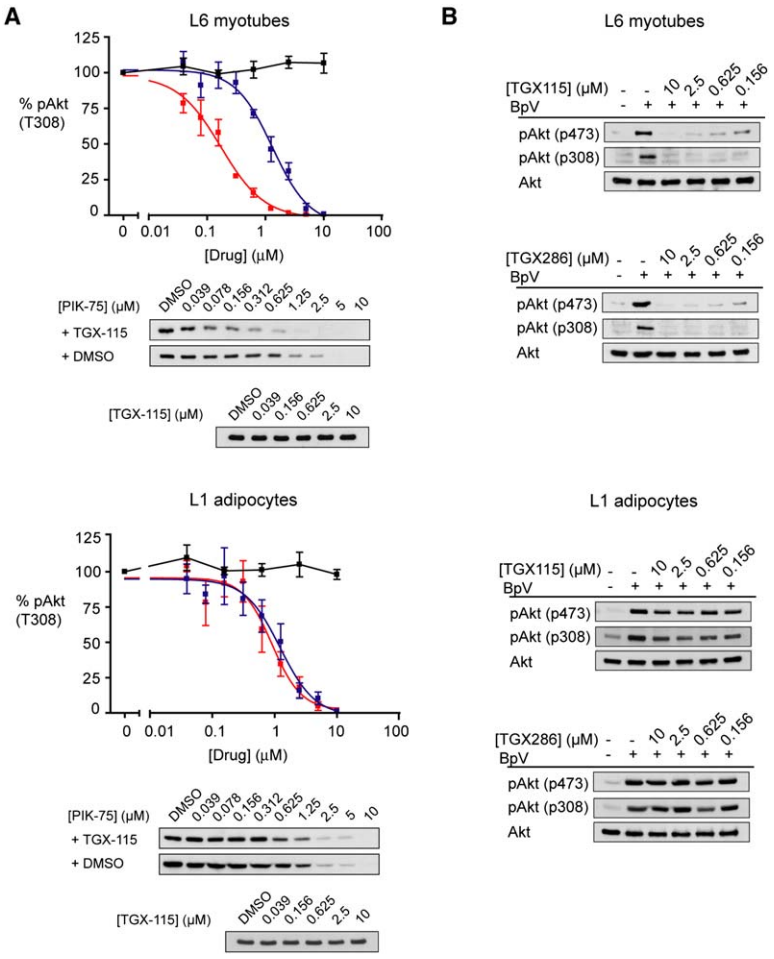

Figure 7. p110β Sets a Threshold for p110α Activity in Myotubes, but Not Adipocytes

(A) Dose response for inhibition of Akt Thr 308 phosphorylation in response to TGX-115 (black), PIK-75 (blue), or PIK-75 + 10 μM TGX-115 (red) in adipocytes or myotubes. Representative Western blots are shown below. Error bars represent mean ± SEM.

(B) Effect of the p110β inhibitors TGX-115 and TGX-286 on Akt phosphorylation induced by the PTEN inhibitor bpV(pic) (5 μM).

Addressing these questions will require a systematic reinterpretation of PI3-K signaling based on pharmacological inhibitors with defined isoform-selectivities. Toward this goal, we report here the biochemical and structural analysis of a panel of potent, chemotypically diverse, and isoform-selective inhibitors of the PI3-K family. This family-wide selectivity analysis provides the first global view of the interaction between chemically diverse inhibitors and the PI3-K family, revealing pairs of kinases (pharmalogs) that display similarities in inhibitor sensitivity not predicted by sequence analysis. As this inhibitor array includes representatives from a large number of chemotypes currently in preclinical development, these compounds preview the target selectivities, and therefore biological activities, of eventual clinical candidates.

The crystal structure of PIK-39 provides the first structural rationale for selective inhibition of a lipid kinase, based on the identification of an active site residue (Met 804) that undergoes an inhibitor-induced conformational rearrangement to create a novel selectivity pocket. This insight should guide the design of selective PI3-K inhibitors, in the same way that structural studies of the gatekeeper pocket (Schindler et al., 1999) and the inactive conformation (Schindler et al., 2000) have guided the discovery of selective protein kinase inhibitors. Alternative mechanisms of inhibitor selectivity are likely to be important for other PI3-K family members, and the structure of a novel inhibitor with selectivity for p110γ has recently been reported (Camps et al., 2005). This crystal structure may assist in the design of p110γ inhibitors, although the features that control the isoform-selectivity of this compound have not been described.

The key role of PI3-K in insulin signaling raises concerns about the therapeutic use of PI3-K inhibitors, and we therefore explored the sensitivity of insulin signaling to pharmacological inhibition of different PI3-Ks. This analysis identified p110α as the critical lipid kinase required for insulin signaling in two key cell types, adipocytes and myotubes. p110β and p110δ, by contrast, play a secondary role in insulin signaling in these cells. p110β and p110δ are being actively pursued as targets for the treatment of thrombosis and inflammation, respectively, and our results suggest that insulin resistance is less likely to be associated with drugs that inhibit these enzymes. p110α inhibitors are more likely to block insulin signaling, but it is important to emphasize that we have focused in this

report only on the effects of acute insulin and drug treatment. As glucose homeostasis involves complex and dynamic signaling across tissues, it will be important to investigate the effects of chronic inhibitor treatment in vivo and correlate these effects with the detailed target selectivity, dosing regimen, and pharmacokinetics of different inhibitors. Likewise, we have focused on target tissues such as fat and muscle that control glucose clearance from the blood, but glucose metabolism in the liver is also regulated by insulin, and the PI3-K inhibitor sensitivity of this process remains unexplored. These questions may begin to be addressed using the chemical array reported here.

Translating our detailed knowledge of signal transduction into effective targeted therapies is a key challenge for biomedical research. Pharmacology will play an important role in meeting this challenge, not least because small molecules often induce emergent phenotypes that cannot be anticipated from the isolated study of their targets (Knight and Shokat, 2005). We have described here a novel approach for pharmacological target validation, based on the parallel evaluation of chemotypically diverse inhibitors whose targets span a protein family and the correlation of the activity of these compounds with their detailed biochemical target selectivity.

EXPERIMENTAL PROCEDURES

Synthesis and Biochemical Characterization of PI3-K Inhibitors

PI3-K inhibitors were synthesized following published patent specifications (Barvian et al., 2004; Bruce et al., 2003; Halbrook et al., 2002; Hayakawa et al., 2003a, 2003b; Jackson et al., 2004; Robertson et al., 2001; Sadhu et al., 2001; Shimada et al., 2004; Smith et al., 2003). Inhibitors for which an alternative designation was not known are denoted "PIK-XXX." Protein and lipid kinases were expressed, purified, and subjected to in vitro kinase assays to determine IC_{50} values. See Supplemental Experimental Procedures for additional details.

Determination of p110γ Crystal Structures

Recombinant human p110γ (residues 144–1102, with a His_6 tag directly fused to the C terminus) was purified from baculovirus-infected Sf9 cells. Crystals were grown at 17°C using sitting-drop vapor diffusion, and these crystals were soaked with inhibitor. Diffraction data was collected at ESRF ID14-4. Data collection and refinement statistics are summarized in Table S2. See Supplemental Experimental Procedures for additional details.

PI3-K Pathway Western Blotting

Adipocytes or myotubes were serum-starved overnight. Cells were then preincubated with inhibitor (30 min), stimulated with insulin (100 nM, 5 min), and lysed. These lysates were resolved by SDS-PAGE, transferred to nitrocellulose, and analyzed by Western blotting.

^{32}P-Orthophosphate Lipid Profiling

Metabolic labeling was performed essentially as described (Serunian et al., 1991). Cells were serum-starved overnight, incubated in phosphate-free medium (2 hr), and then labeled (2 hr) with ^{32}P-orthophosphate. After this labeling, inhibitors were added to their final concentration (10 min) and then treated with insulin (100 nM, 10 min). Cells were lysed, the lipids extracted and deacylated, and analyzed by HPLC.

Glucose Uptake

Glucose uptake in adipocytes was measured essentially as described (Lakshmanan et al., 2003). Adipocytes in 12-well plates were serum-starved (3 hr) and then incubated in PBS with compound (30 min), at which point cells were stimulated with insulin (100 nM). (^{3}H)-2-deoxyglucose (100 μM,1 μCi/ml) was added 15 min after insulin stimulation and uptake was allowed to proceed for an additional 15 min. Adipocytes were washed three times with PBS, dissolved in 0.1% SDS, and the internalized radioactivity was measured by scintillation counting.

Insulin-Tolerance Tests

Four-month-old FVB/N female mice (n = 5) were fasted at 9:00 a.m. and then given human insulin (Sigma, 0.75 U/kg) or vehicle (PBS) intravenously at 12:00 p.m. on the same day. Immediately following insulin treatment, animals were given an intraperitoneal injection of inhibitor (10 mg/kg) or vehicle (50% DMSO). Blood glucose level was measured with an Accu-Check Active glucose meter at 15 min intervals after insulin injection.

Supplemental Data

Supplemental Data include six figures, three tables, four movies, and Supplemental Experimental Procedures and can be found with this article online at http://www.cell.com/cgi/content/full/125/4/733/DC1/.

ACKNOWLEDGMENTS

Z.A.K. is an HHMI Predoctoral Fellow. We thank the Sandler Program in Basic Sciences and in Asthma Research, NIH AI44009, and the Brain Tumor Society for funding. B.G. was supported by a fellowship from Secretaría de Estado de Educación y Universidades and cofinanced by the European Social Fund. T.B, A.B, and B.T. were supported by the Intramural Research Program of the NICHD of the National Institutes of Health. R.L.W. was supported by the Medical Research Council. We acknowledge the ESRF for provision of synchrotron radiation facilities and thank Ingar Leiros for assistance with beamline ID14-4.

Received: September 6, 2005
Revised: February 6, 2006
Accepted: March 15, 2006
Published online: April 27, 2006

REFERENCES

Alaimo, P.J., Knight, Z.A., and Shokat, K.M. (2005). Targeting the gatekeeper residue in phosphoinositide 3-kinases. Bioorg. Med. Chem. *13*, 2825–2836.

Asano, T., Kanda, A., Katagiri, H., Nawano, M., Ogihara, T., Inukai, K., Anai, M., Fukushima, Y., Yazaki, Y., Kikuchi, M., et al. (2000). p110beta is up-regulated during differentiation of 3T3–L1 cells and contributes to the highly insulin-responsive glucose transport activity. J. Biol. Chem. *275*, 17671–17676.

Barvian, N.C., Kolz, C.N., Para, K.S., Patt, W.C., and Viskick, M. June 2004. Benzoxazin-3-ones and derivatives thereof as inhibitors of PI3K. WO 04/052373.

Bi, L., Okabe, I., Bernard, D.J., Wynshaw-Boris, A., and Nussbaum, R.L. (1999). Proliferative defect and embryonic lethality in mice homozygous for a deletion in the p110alpha subunit of phosphoinositide 3-kinase. J. Biol. Chem. *274*, 10963–10968.

Bi, L., Okabe, I., Bernard, D.J., and Nussbaum, R.L. (2002). Early embryonic lethality in mice deficient in the p110beta catalytic subunit of PI 3-kinase. Mamm. Genome *13*, 169–172.

Brachmann, S.M., Ueki, K., Engelman, J.A., Kahn, R.C., and Cantley, L.C. (2005). Phosphoinositide 3-kinase catalytic subunit deletion and regulatory subunit deletion have opposite effects on insulin sensitivity in mice. Mol. Cell. Biol. *25*, 1596–1607.

Bruce, I., Finan, P., Leblanc, C., McCarthy, C., Whitehead, L., Blair, N., Bloomfield, G., Hayler, J., Kirman, L., Oza, M., and Shukla, L. September 2003. 5-phenylthiazole derivatives and use as PI3 kinase inhibitors. WO 03/072557.

Camps, M., Ruckle, T., Ji, H., Ardissone, V., Rintelen, F., Shaw, J., Ferrandi, C., Chabert, C., Gillieron, C., Francon, B., et al. (2005). Blockade of PI3Kgamma suppresses joint inflammation and damage in mouse models of rheumatoid arthritis. Nat. Med. *11*, 936–943.

Cantley, L.C., and Neel, B.G. (1999). New insights into tumor suppression: PTEN suppresses tumor formation by restraining the phosphoinositide 3-kinase/AKT pathway. Proc. Natl. Acad. Sci. USA *96*, 4240–4245.

Condliffe, A.M., Davidson, K., Anderson, K.E., Ellson, C.D., Crabbe, T., Okkenhaug, K., Vanhaesebroeck, B., Turner, M., Webb, L., Wymann, M.P., et al. (2005). Sequential activation of class IB and class IA PI3K is important for the primed respiratory burst of human but not murine neutrophils. Blood *106*, 1432–1440.

Domin, J., and Waterfield, M.D. (1997). Using structure to define the function of phosphoinositide 3-kinase family members. FEBS Lett. *410*, 91–95.

Fan, Q.-W., Knight, Z.A., Goldenberg, D.D., Yu, W., Mostov, K.E., Stokoe, D., Shokat, K.M., and Weiss, W.A. (2006). A dual PI3-kinase/mTOR inhibitor reveals emergent efficacy in glioma. Cancer Cell *9*, 341–349.

Feng, J., Park, J., Cron, P., Hess, D., and Hemmings, B.A. (2004). Identification of a PKB/Akt hydrophobic motif Ser-473 kinase as DNA-dependent protein kinase. J. Biol. Chem. *279*, 41189–41196.

Fruman, D.A., Meyers, R.E., and Cantley, L.C. (1998). Phosphoinositide kinases. Annu. Rev. Biochem. *67*, 481–507.

Halbrook, J., Kesicki, E., Burgess, L.E., Schlachter, S.T., Eary, C.T., Schiro, J.G., Huang, H., Evans, M., and Han, Y. March 2002. Materials and methods to potentiate cancer treatment. WO 02/20500.

Harrington, L.S., Findlay, G.M., and Lamb, R.F. (2005). Restraining PI3K: mTOR signalling goes back to the membrane. Trends Biochem. Sci. *30*, 35–42.

Hayakawa, M., Kaizawa, H., Kawaguchi, K., Matsuda, K., Ishikawa, N., Koizumi, T., Yamano, M., Okada, M., Ohta, M. January 2003a. Imidazopyridine derivatives. European patent 1,277,754.

Hayakawa, M., Kaizawa, H., Moritoma, H., Kawaguchi, K., Koizumi, T., Yamano, M., Matsuda, K., Okada, M., Ohta, M. January 2003b. Condensed heteroaryl derivatives. European patent 1,277,738.

Hickson, I., Zhao, Y., Richardson, C.J., Green, S.J., Martin, N.M., Orr, A.I., Reaper, P.M., Jackson, S.P., Curtin, N.J., and Smith, G.C. (2004). Identification and characterization of a novel and specific inhibitor of the ataxia-telangiectasia mutated kinase ATM. Cancer Res. *64*, 9152–9159.

Jackson, S.P., Robertson, A.D., Kenche, V., Thompson, P., Prabaharan, H., Anderson, K., Abbott, B. Goncalves, I., Nesbitt, W., Shoenwaelder, S., and Saylik, D. February 2004. Inhibition of phosphoinositide 3-kinase beta. WO 04/016607.

Jackson, S.P., Schoenwaelder, S.M., Goncalves, I., Nesbitt, W.S., Yap, C.L., Wright, C.E., Kenche, V., Anderson, K.E., Dopheide, S.M., Yuan, Y., et al. (2005). PI 3-kinase p110beta: a new target for antithrombotic therapy. Nat. Med. *11*, 507–514.

Katso, R., Okkenhaug, K., Ahmadi, K., White, S., Timms, J., and Waterfield, M.D. (2001). Cellular function of phosphoinositide 3-kinases: implications for development, homeostasis, and cancer. Annu. Rev. Cell Dev. Biol. *17*, 615–675.

Knight, Z.A., and Shokat, K.M. (2005). Features of selective kinase inhibitors. Chem. Biol. *12*, 621–637.

Knight, Z.A., Chiang, G.G., Alaimo, P.J., Kenski, D.M., Ho, C.B., Coan, K., Abraham, R.T., and Shokat, K.M. (2004). Isoform-specific phosphoinositide 3-kinase inhibitors from an arylmorpholine scaffold. Bioorg. Med. Chem. *12*, 4749–4759.

Lakshmanan, J., Elmendorf, J.S., and Ozcan, S. (2003). Analysis of insulin-stimulated glucose uptake in differentiated 3T3-L1 adipocytes. Methods Mol. Med. *83*, 97–103.

Lau, A., Swinbank, K.M., Ahmed, P.S., Taylor, D.L., Jackson, S.P., Smith, G.C., and O'Connor, M.J. (2005). Suppression of HIV-1 infection by a small molecule inhibitor of the ATM kinase. Nat. Cell Biol. *7*, 493–500.

Luo, J., Field, S.J., Lee, J.Y., Engelman, J.A., and Cantley, L.C. (2005). The p85 regulatory subunit of phosphoinositide 3-kinase down-regulates IRS-1 signaling via the formation of a sequestration complex. J. Cell Biol. *170*, 455–464.

Madhusudan, Trafny, E.A., Xuong, N.H., Adams, J.A., Teneyck, L.F., Taylor, S.S., and Sowadski, J.M. (1994). cAMP-dependent protein-kinase—crystallographic insights into substrate recognition and phosphotransfer. Protein Sci. *3*, 176–187.

Patrucco, E., Notte, A., Barberis, L., Selvetella, G., Maffei, A., Brancaccio, M., Marengo, S., Russo, G., Azzolino, O., Rybalkin, S.D., et al. (2004). PI3Kγ modulates the cardiac response to chronic pressure overload by distinct kinase-dependent and -independent effects. Cell *118*, 375–387.

Peng, Y., Woods, R.G., Beamish, H., Ye, R., Lees-Miller, S.P., Lavin, M.F., and Bedford, J.S. (2005). Deficiency in the catalytic subunit of DNA-dependent protein kinase causes down-regulation of ATM. Cancer Res. *65*, 1670–1677.

Robertson, A.D., Jackson, S., Kenche, V., Yaip, C., Parbaharan, H., and Thompson, P. July 2001. Therapeutic morpholino-substituted compounds. WO 01/53266.

Ruderman, N.B., Kapeller, R., White, M.F., and Cantley, L.C. (1990). Activation of phosphatidylinositol 3-kinase by insulin. Proc. Natl. Acad. Sci. USA *87*, 1411–1415.

Sadhu, C., Dick, K., Treiberg, J., Sowell, C., Kesicki, E.A., and Oliver, A. April 2001. Inhibitors of human phosphatidyl-inositol 3-kinase delta. WO 01/81346.

Sadhu, C., Masinovsky, B., Dick, K., Sowell, C.G., and Staunton, D.E. (2003). Essential role of phosphoinositide 3-kinase delta in neutrophil directional movement. J. Immunol. *170*, 2647–2654.

Samuels, Y., Wang, Z., Bardelli, A., Silliman, N., Ptak, J., Szabo, S., Yan, H., Gazdar, A., Powell, S.M., Riggins, G.J., et al. (2004). High frequency of mutations of the PIK3CA gene in human cancers. Science *304*, 554.

Schindler, T., Sicheri, F., Pico, A., Gazit, A., Levitzki, A., and Kuriyan, J. (1999). Crystal structure of Hck in complex with a Src family-selective tyrosine kinase inhibitor. Mol. Cell *3*, 639–648.

Schindler, T., Bornmann, W., Pellicena, P., Miller, W.T., Clarkson, B., and Kuriyan, J. (2000). Structural mechanism for STI-571 inhibition of abelson tyrosine kinase. Science *289*, 1938–1942.

Schmid, A.C., Byrne, R.D., Vilar, R., and Woscholski, R. (2004). Bisperoxovanadium compounds are potent PTEN inhibitors. FEBS Lett. *566*, 35–38.

Serunian, L.A., Auger, K.R., and Cantley, L.C. (1991). Identification and quantification of polyphosphoinositides produced in response to platelet-derived growth factor stimulation. Methods Enzymol. *198*, 78–87.

Shimada, M., Murata, T., Fuchikami, K., Tsujishita, H., Omori, N., Kato, I., Miura, M., Urbahns, K., Gantner, F., and Bacon, K. April 2004. Fused azole-pyrimidine derivatives. WO 04/029055.

Smith, G.C., Martin, N.M., Jackson, S.P., O'Connor, M.J., Lau, A.Y., Cockcroft, X.F., Matthews, I.T., Menear, K.A., Rigoreau, L.J., Hummerson, M.G., and Griffin, R.J. August 2003. Pyranones useful as ATM inhibitors. WO 03/070726.

Ueki, K., Yballe, C.M., Brachmann, S.M., Vicent, D., Watt, J.M., Kahn, C.R., and Cantley, L.C. (2002). Increased insulin sensitivity in mice lacking p85beta subunit of phosphoinositide 3-kinase. Proc. Natl. Acad. Sci. USA *99*, 419–424.

Ueki, K., Fruman, D.A., Yballe, C.M., Fasshauer, M., Klein, J., Asano, T., Cantley, L.C., and Kahn, C.R. (2003). Positive and negative roles of p85 alpha and p85 beta regulatory subunits of phosphoinositide 3-kinase in insulin signaling. J. Biol. Chem. *278*, 48453–48466.

Vanhaesebroeck, B., Ali, K., Bilancio, A., Geering, B., and Foukas, L.C. (2005). Signalling by PI3K isoforms: insights from gene-targeted mice. Trends Biochem. Sci. *30*, 194–204.

Viniegra, J.G., Martinez, N., Modirassari, P., Losa, J.H., Parada Cobo, C., Lobo, V.J., Luquero, C.I., Alvarez-Vallina, L., Ramon y Cajal, S., Rojas, J.M., and Sanchez-Prieto, R. (2005). Full activation of PKB/Akt in response to insulin or ionizing radiation is mediated through ATM. J. Biol. Chem. *280*, 4029–4036.

Walker, E.H., Perisic, O., Ried, C., Stephens, L., and Williams, R.L. (1999). Structural insights into phosphoinositide 3-kinase catalysis and signalling. Nature *402*, 313–320.

Walker, E.H., Pacold, M.E., Perisic, O., Stephens, L., Hawkins, P.T., Wymann, M.P., and Williams, R.L. (2000). Structural determinants of phosphoinositide 3-kinase inhibition by wortmannin, LY294002, quercetin, myricetin, and staurosporine. Mol. Cell *6*, 909–919.

Ward, S., Sotsios, Y., Dowden, J., Bruce, I., and Finan, P. (2003). Therapeutic potential of phosphoinositide 3-kinase inhibitors. Chem. Biol. *10*, 207–213.

Yart, A., Roche, S., Wetzker, R., Laffargue, M., Tonks, N., Mayeux, P., Chap, H., and Raynal, P. (2002). A function for phosphoinositide 3-kinase beta lipid products in coupling beta gamma to Ras activation in response to lysophosphatidic acid. J. Biol. Chem. *277*, 21167–21178.

Yu, J., Zhang, Y., McIlroy, J., Rordorf-Nikolic, T., Orr, G.A., and Backer, J.M. (1998). Regulation of the p85/p110 phosphatidylinositol 3′-kinase: stabilization and inhibition of the p110alpha catalytic subunit by the p85 regulatory subunit. Mol. Cell. Biol. *18*, 1379–1387.

Accession Numbers

Atomic coordinates and structure factors are deposited in the Protein Data Bank with accession codes 2chw (PIK-39), 2chx (PIK-90), and 2chz (PIK-93).